Observations of 6cm OH Maser Emission in MonR2 and LDN 1084

Laura Zschaechner, Nguyen Phan

May 11, 2009

Abstract

MonR2 and LDN 1084, both regions of massive star formation, are known sources of excited state OH maser emission at the 4765 MHz transition. Both of these sources have been studied over the past 20-25 years and have displayed variability over time. In this paper, we give a brief overview of the phenomenon of astrophysical masers and discuss additional observations made with the VLA at 4765 MHz which could be used to better characterize variability of these two sources. We report a detection of approximately 6.65 Jy in MonR2, but due to a pointing error, no detection was made for LDN 1084. Our observed flux density for MonR2 suggests that it might be undergoing another flaring event. However, frequent observations are needed to better characterize the variability of this maser

1 Introduction

1.1 Background on Masers

The discovery of the first astrophysical maser dates back to 1965 when Weaver et al. detected 1665 MHz emission emanating from a region of star formation (Gray). The initial discovery caused bewilderment and the molecule responsible for the emission was labeled 'mysterium' (Gray). However, polarization measurements conducted by Weinre et al. (1965) identified the 1665 MHz emission as the result of molecular transitions in OH, the hydroxyl molecule (Elitzur). The invention of the laboratory maser about a decade earlier provided an understanding of the physics of light amplification by stimulated emission and was eventually used to explain mechanism behind astrophysical masers (Letokhov and Johansson). Although the mechanism powering astrophysical masers are similar to that of laboratory masers, astrophysical masers are simpler because of the absence of resonant cavities and reflecting mirrors (Elitzur).

Today, over one hundred maser species have been discovered in interstellar space among these are OH, CO_2, NH_3, H_2O, SiO, HCN, CH, CH_3OH (methanol), and H_2CO (Gray). Table 1 gives a brief overview of several species that have been detected from the radio to the optical regimes and the corresponding year of discovery (Letokohov and Johansson). Maser emission has been found in a wide variety of astrophysical environments. Galactic masers are typically found in comets, molecular clouds, star-forming regions, the circumstellar envelopes of late-type stars, supernovae remnants expanding into adjacent molecular region, and even in planetary atmospheres (Letokhov and Johansson). Their extragalactic counterparts, referred to as megamersars because of their high luminosities, are found near the jets and nuclei of active galaxies (Letokhov and Johansson).

– microwaves	molecules	OH, 18.5 cm H_2O, 1.35 cm	Weaver *et al.*, 1965 Cheung *et al.*, 1969
	> 100 molecular species		Townes, 1997
– submillimeters	atom	H^{**}	Strelnitskii *et al.*, 1996
– IR	molecule (Mars, Venus)	CO_2, 10 µm	Johnson *et al.*, 1976 Mumma *et al.*, 1981
– optical waves	ion, atom	$Fe^+ \simeq 1$ µm O I, 8446 Å	Johansson, Letokhov, 2002, 2003*a*
	Eta Carinae, gas condensations		Johansson, Letokhov, 2005*c*

Table 1: A table listing several maser species that have been discovered in interstellar space and the corresponding year of discovery (Litokhov & Johansson).

Regardless of the masing species and the environments that they are found in, masers tend to exhibit several common properties such as high variability in the observed flux density, Doppler broadening of spectral lines due to thermal motions, the narrowing of spectral line components due to amplification, and extremely high brightness temperatures (Gray). The high brightness temperature, which can range from 10^4 K to over 10^14 K, is one of the primary reasons why maser emission cannot be thermal and must be result of stimulated emission. At 10^14 K, a temperature over a million times hotter than the Sun's core, molecules would dissociate and consequently spectral line emission arising from molecular transitions cannot occur.

Because maser radiation is due to amplification by stimulated emission, a population inversion in the gain medium must be provided by a pumping source. The three pumping sources that can create a population inversion are collisions resulting from stellar winds or shockwaves, non-thermal radiation, particularly from infra-red photons re-emitted by dust particles, and chemical reactions responsible for the creation of the molecules, which can leave them in the excited state (Thompson). The pumping mechanisms, which can differ as a result of the diverse environments in which masers are found, is a subject of great interest and continuing research.

Although more research is needed to elucidate the pumping mechanisms behind masers, the study of masers have provided much information about their surrounding environments and could potentially have cosmological as well as some unconventional applications. Because many masers such as MonR2 and LDN 1084 occur in star forming regions, analysis of their spectral lines and polarization can give estimates of the magnetic field strengths, temperatures, densities, and compositions of these regions. When masers occur in the envelopes of late-type stars, the time lag between the changes in the starlight and the maser emission can be used determine the size of the envelope, and hence the distance to the maser (Gray). In the case of megamasers, which are found in the clouds surrounding active galactic nuclei, the rotational speeds of these masers derived from shifts in their spectral lines have been used to estimate the mass of the central black hole (e.g. NGC4258) (Gray). Observations of megamasers at high redshifts can be conducted to study chemical abundances in the early universe, and maser emission could also have potential applications to the search for extra-solar planets and SETI (Gray).

1.2 OH Maser Pumping

The pumping scheme for excited state OH maser emission remains undetermined although some constraints have been made (Gray 2007). It is believed that the environment surrounding and within the maser play a significant role in whether or not the material will mase. Absorption of specific wavelengths of radiation is also thought to trigger excited state transitions which lead to a population inversion. One factor which needs to be considered in order to better understand the pumping mechanism of excited OH maser emission is the variability over time. Observations of the variability may help to put additional constraints on the model for the pumping mechanism of OH maser emission in not only the excited states, but the ground states as well in star forming regions. In order to potentially observe this variability, we have chosen to observe two star forming regions which have exhibited maser emission in both the ground and excited states: MonR2 and LDN 1084.

1.3 MonR2 and LDN 1084

Observations of MonR2 date back to 1983 when it was detected by Gardiner and Martin-Pintado. MonR2 was then observed at one to two week intervals from 1995 to 1998 by Smits et al.. During this time the maser experienced two flaring events, one of which peaked at 30 Jy and the other nearing 80 Jy (Smits et al. 1998). However, as of December 1998, there were no detections of maser emission at 4.7 GHz and observations continued into November of 2001 (Smits et al. 2003). Additional observations made in 2002 by Harvey-Smith & Cohen (2005) also found no detections. But, in May of 2006, a detection was made at 5 Jy with a central velocity of approximately 10.5 km/s. This detection was consistent with the average central velocitiy of around 10.7 km/s observed by Smits et al.. This redetection of maser emission in MonR2 may indicate that the maser is experiencing the beginning (or end) of a new flaring event and is the motivating factor for our observations.

LDN 1084, another massive star forming region first observed in 1988 (Cohen et al. 1988) has shown substantial variability, though not as dramatic as MonR2, during subsequent observations over the past 20 years, decreasing from 700 mJy

(Cohen et al. 1991, 1995) to 480 mJy (Harvey-Smith & Cohen 2005) and then showing a potential flare of around 1 Jy in 2006 (Fish et al. 2006). In addition to the maser sources, the aforementioned star forming region MonR2 has also itself been an object of study.

Previous observations of LDN 1084 using the VLA have been made. In 1994, Miralles et al. observed the 2 and 6 cm lines. Unfortunately, aside from the abstract, this article is no longer available. What we can conclude from this is that there was a detection at that time. Observations of the star forming region LDN 1084 have also been made at other wavelengths. In 2003, it was observed in the infrared by Venkataraman & Anandarao using the 1.2 m PRL Infrared Telescope. It was also observed in the 2 Micron All Sky Survey (2Mass). According to the 2003 observations, the central structure was missed, but detected by 2MASS. This is merely due to differences in the wavelengths observed as the 2003 observations were done in the H and K' bands and 2Mass was done using the J band.

2 Observations

Observations were made on February 21, 2009 using the VLA in B configuration with 27 antennas. The 4765.562 MHz transition of OH was observed with a bandwidth of 2.3 MHz divided into128 spectral channels, giving a channel spacing of 17.97 kHz (1.13 km/s). The total time on source was approximately 11 minutes for MonR2 and 10 minutes for LDN 1084. Absolute flux calibration was done with 3C48 (0137+331) and phase calibration was done using 0607-085 for MonR2 and 0016-002 for LDN 1084. Dopset was not used at the time of observations.

3 Analysis

Data reduction was done using the Astronomical Image Processing System (AIPS). Before calibration, antenna 15 was flagged using TVFLG for the entire duration of data taking. There were no significant sources of radio frequency interference and minimal flagging was done otherwise. There was however, one spot of bad data which appeared on the visibility plot for MonR2 and we were unable to remove.

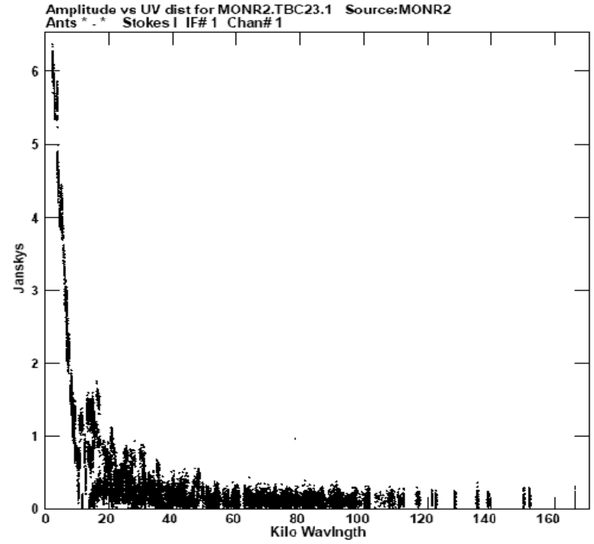

Figure 1: The visibility data for MonR2. We were unable to remove a single point of bad data at a baseline of approximately 80 kλ.

Following the initial editing, SETJY was used in order to obtain the flux for 3C48. This was found to be 5.5348 Jy for the MonR2 observations and 5.527 Jy for the LDN 1084 observations, which were comparable to the value of 5.48 Jy found in the calibrator manual for 3C48 at this frequency.

Following SETJY, CALIB was used with antenna 11 as a reference antenna. The UV range was set to 0, 50 for 3C48 and 0, 0 for the phase calibrators.

Using GETJY the flux of 0607-085 was found to be approximately 1.10314 Jy and the flux of 0016+002 was 0.52941 Jy.

In order to obtain a map, IMAGR was used and then self calibration was applied.

For the initial map of MonR2, the rms noise was 2.5259 mJy/beam. Through five iterations of self-calibration the rms noise was brought down to 0.82512 mJy/beam, which was approximately 3 mJy/beam (40%) higher than the theoretical noise of 0.509249 mJy/beam, which was calculated using the online VLA thermal noise calculator.

Self-calibration as not applied to LDN 1084 and the final rms noise was found to be 1.6194 mJy/beam. This is considerably higher than the theoretical noise of 0.5090249 mJy/beam, but lower than the noise for the initial map of MonR2.

The reason for these discrepancies is that there was no detection at this stage, so naturally, the rms noise would be lower initially, but without self-calibration no improvement was made.

An image cube was made for each source by first copying the calibration, flag and solution tables from the channel zero data into the line data using TACOP. If done incorrectly, this will result in uncalibrated image cubes.

The initial image cubes for both sources were uncalibrated, which for LDN 1084 resulted in an rms noise less than the theoretical. For the MonR2 data, the source was initially unrecognizable, but appeared as six bright flashes in selected channels. Upon correction, the rms noise reached a reasonable value for both sources and the sources in MonR2 became clear. Following the making of the image cubes, JMFIT was used in order to make a Gaussian of the maser source.

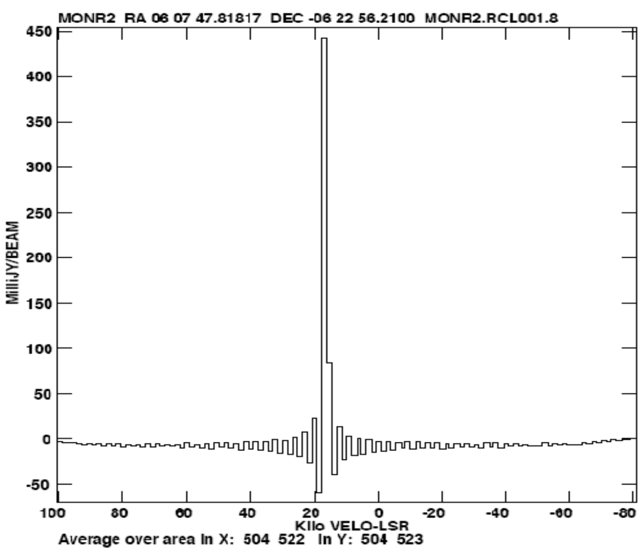

Figure 2: The MonR2 spectrum displaying Gibbs ringing, which was removed by applying Hanning smoothing.

In addition to this, ISPEC was used in order to obtain a spectrum of the maser in MonR2. Initially, there was substantial Gibbs ringing, which was dealt with by applying Hanning smoothing. Following this, the maser appeared to spread over four channels and was examined in each. In order to obtain the velocities, CVEL was used with the aid of the online dopset tool.

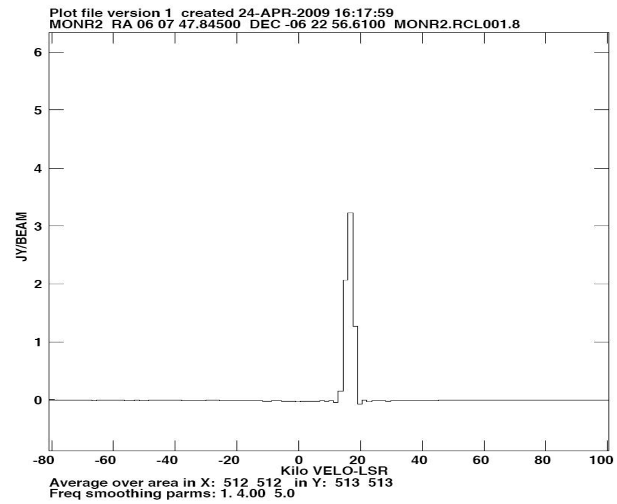

Figure 3: The MonR2 spectrum with Hanning smoothing applied. The maser emission is spread over four channels with the peak emission in channel 55 centered at 9.043 km/s.

4 Results

4.1 Detections

For the source MonR2 we made a detection with a peak of $3.2286 \pm 5.94 \times 10^{-3}$ Jy at 4765.771 MHz spanning four channels. The velocity of the peak channel was 9.043 km/s. In the next channel up, a detection of $2.062 \pm 5.49 \times 10^{3}$ Jy was made. Possible faint emission in the following channel was detected at a level of $0.103083 \pm 4.98 \times 10^{-3}$ Jy. Furthermore, in the channel directly below the peak, $1.2542 \pm 5.21 \times 10^{-3}$ Jy was recorded. The total maser emission was determined to be approximately 6.65 Jy by adding the flux densities in the four channels.

The maser emission was located at 06h 07m 46.15s -06 deg 23' 05.64", which is consistent to within ten arcseconds of the emission observed by Fish et al. in 2006 (06h 07m 47.845s, -06 deg 22' 56.61"). The central velocity is also within a reasonable range in comparison to the 10.4 km/s and 10.62 km/s velocities of the emission from two channels. We were able to model the maser emission with a Gaussian in order to obtain an angular size of $7.73661 \pm 0.32321''$ for the major axis and $1.33692 \pm 0.15790''$ for the minor axis. Using this angular size and the flux density, the brightness temperature of the maser emission was calculated to be 4.06×10^{3} K. This leads us to conclude that this is a fairly weak maser. It is unlikely that the angular size created in the model is incorrect as it appears to match well with the size obtained by examining the contour plot of the maser and adjacent HII region.

If one calculates the brightness temperature for the 80 Jy flare observed by Smits et al., one will only find a brightness temperature of 4.8×10^4 Jy. While this is considerably higher than the value we obtained, it is still quite low relative to the typical brightness temperatures of masers.

The rms noise in the central channel of the maser, being at roughly 0.8 mJy was slightly higher than that of the other channels (0.56 mJy). This was likely due to a calibration error, which may be corrected in the individual channel, but due to time constraints has not been done.

While the primary goal of this observation was to gain information concerning the status of the maser, MonR2 itself was also observed. The angular size was approximately 30" and the peak flux was approximately 96 mJy and a total flux of approximately 8.4 Jy, yielding a brightness temperature of 570 K.

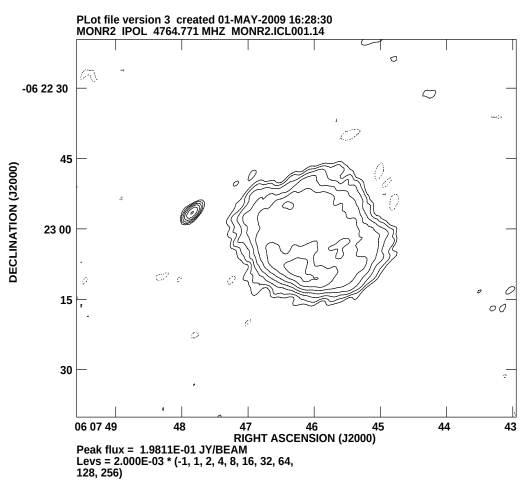

Figure 4: A contour plot of the MonR2 maser and the adjacent HII region. The positive contours are separated by powers of two with a corresponding peak flux of 1.9811×10^-1 Jy/beam

In the process of analyzing the map of LDN 1084, it was noticed that the VLA was not actually directed towards LDN 1084, but rather in a different part of the sky entirely. However, the beam was relatively close to a known quasar.

5 Discussion

5.1 MonR2 - Maser

Our observations found a flux density of 6.7 Jy, a value which is low in comparison to the 80 Jy flare observed by Smits et al.. Although this indicates only a small variability since the last observations were performed in 2006 by Fish et al. which found a value of 5 Jy, it does not necessarily rule out significant variability at 4765 MHz over the three years that MonR2 were not observed. It is possible that the flux has remained relatively constant during this time, or that there have been multiple flares. Naturally, frequent observations are necessary in order to put constraints on models for excited state OH maser emission from star forming regions. The maser in MonR2 could quite possibly be experiencing the beginning or end of yet another flaring event. But these subsequent flares might be lower in amplitude than the previous 30 Jy and 80 Jy flares due to a degradation in the conditions necessary to induce maser emission.

One must also consider the possibility of a trend leading away from variability and resulting in a stabilization of the maser emission. Naturally, this emission would be of a lower magnitude than that of the peak flares and could result in a median value or perhaps degrade over time as well. Of course, this is mainly speculation as observations must be made more frequently in order to put constraints on the variability and a greater sample size is necessary in order to put constraints on the pumping model for OH in star forming regions.

5.2 MonR2 - Star Forming Region

Although it is not the primary topic of this paper, the star forming region MonR2 itself has previously been observed at this frequency as well as others (Massi et al. 1985). In 1985, it was observed at 6 cm, but the exact frequency was unspecified. This previous observation was also done using 3C48 as a calibrator and a configuration close to B. The upper limit on the flux density was 1mJy/bm, which is significantly lower than our detection of approximately 100 mJy/bm. This discrepancy may be due to a difference in the frequencies used. In companion with their 6 cm observations, Massi et al. observed at 1.3 cm in

D configuration and detected a peak flux density of 1.2 mJy/bm. Once again, the exact frequency was not given.

Outside of the radio regime, MonR2 was also observed in the near-infrared at several different wavelengths as well as in the continuum. (Howard et al. 1994)

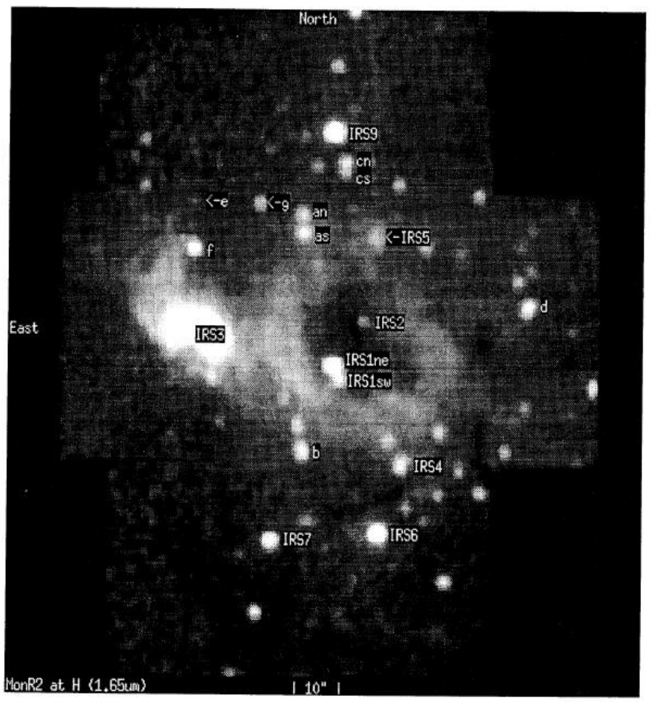

Figure 5: An image of MonR2 at 1.65 μm. (Howard et al. 1994)

Figure 6: An image of r the Brα (n=5$\rightarrow 4, 4.052\mu$ m) line minus continuum. (Howard et al. 1994)

Upon examination of these images, it is apparent that the radio image we obtained is substantially different from the continuum image. However, when the continuum is subtracted from a spectral line image, there is a strong resemblance in both overall shape as well as angular size.

5.3 LDN 1084 - Where We Actually Pointed

While LDN 1084 itself was not observed, the coordinates at which the VLA pointed were very close to a recently discovered quasar of redshift 2.3657 and a magnitude of approximately 20. The coordinates of this quasar are 23h 59h 26.16s, -00 deg 02' 04.9", which would place it near the center of our beam. However, given the high redshift of this object as well as its visual magnitude, we cannot really say much about the nature of its radio emission at 4765 MHz based on 11 minutes of VLA time. Furthermore not much is known concerning this quasar as its detection was first published in the 2007 SDSS Quasar Catalog IV, Fifth Data Release. Radio emission has been observed from approximately 10 percent of quasars, making them radio-loud while the rest only exhibit radio emission which is much less than the optical. (Wadadekar & Kembhavi 1999) As one may assume, this is in agreement with our non-detection.

6 Future Work

Our detection of MonR2 is not enough to put substantial constraints on the variability let alone the OH pumping model in star forming regions. In order to gain additional information concerning the variability, regular observations (every one to two weeks) are necessary. While this may also help establish constraints for the pumping model in these regions, additional observations in the ground state as well as the 6 GHz excited state masers would allow for greater understanding of the physical conditions. Finally, observations of additional star forming regions will be of use in order to obtain a greater sampling and rule out any anomalies observed in MonR2.

7 Acknowledgements

We would like to acknowledge substantial help from Dr. Greg Taylor as well as Steve Tremblay, Esteban Araya and Dr. Ylva Philstrom.

References

Doel, R.C., Gray, M.D., & Field, D., 1990 MNRAS 244 504
Elitzur, M. 1992, Astronomical Masers
Fish et al., 2006, ApJ 653:L45-L48
Gardner, F. F., & Martin-Pintado, J. 1983, A&A, 121, 265
Gray, M. D., 2007, MNRAS, 00, 00
Gray, Malcolm. Phil Trans R Soc A, 1999, 357, 1763
Harvey-Smith, L., & Cohen, R. J. 2005, MNRAS, 356, 637
He, J.H., 2005, arXiv:astro-ph/0502400v1
Howard et al. 1994, ApJ 425, 707
Letokhov, V., Johansson, S. 2009, Astrophysical Lasers
Liu, H.P., Sun, J., Thissen, T., 2004 Ap&SS289, 147
Massi, M., Felli, M., & Simon, M. 1985 A&A, 152, 387
Miralles, M.P., Rodriguez, L.F., & Scalise, E., 1994, ApJS, 92, 173
Pavlakis K.G., Kylafis N.D., 1996, ApJ 467, 300
Schneider et al. 2007 SDSS Quasar Catalog IV. Fifth Data Release
Smits D. P. 2003, MNRAS, 339, 1
Smits, D. P., Cohen, R. J., & Hutawarakorn, B. 1998, MNRAS, 296, L11
Thissen, T., Spiecker, H., Andresen, P., 1999, A&AS 137, 323
Thompson, J.M.T. 2001, Visions of the Future
Venkataraman, V., & Anandarao, B.G. 2005, B.A.S. 33, 141
Wadadekar, Y. & Kembhavi, A. 1999 AJ 118, 1435